Ku-Dependent and Ku-Independent End-Joining Pathways Lead to Chromosomal Rearrangements During Double-Strand Break Repair in *Saccharomyces cerevisiae*

Xin Yu and Abram Gabriel[1]

Department of Molecular Biology and Biochemistry, Rutgers University, Piscataway, New Jersey 08854

Manuscript received September 13, 2002
Accepted for publication November 26, 2002

ABSTRACT

Chromosomal double-strand breaks (DSBs) can be repaired by either homology-dependent or homology-independent pathways. Nonhomologous repair mechanisms have been relatively less well studied, despite their potential importance in generating chromosomal rearrangements. We have developed a *Saccharomyces cerevisiae*-based assay to identify and characterize homology-independent chromosomal rearrangements associated with repair of a unique DSB generated within an engineered *URA3* gene. Approximately 1% of successfully repaired cells have accompanying chromosomal rearrangements consisting of large insertions, deletions, aberrant gene conversions, or other more complex changes. We have analyzed rearrangements in isogenic wild-type, *rad52*, *yku80,* and *rad52 yku80* strains, to determine the types of events that occur in the presence or absence of these key repair proteins. Deletions were found in all strain backgrounds, but insertions were dependent upon the presence of Yku80p. A rare *RAD52*- and *YKU80*-independent form of deletion was present in all strains. These events were characterized by long one-sided deletions (up to 13 kb) and extensive imperfect overlapping sequences (7–22 bp) at the junctions. Our results demonstrate that the frequency and types of repair events depend on the specific genetic context. This approach can be applied to a number of problems associated with chromosome stability.

RECOMBINATIONAL processes are essential for the maintenance of genome stability, for repair of broken DNA and stalled replication forks, for normal meiosis, and for generating diversity in the immune system. In mammals, end joining without regard for homology appears to be the predominant mechanism of double-strand break (DSB) repair, although homologous gene duplication can frequently occur (Liang *et al.* 1998). In *Saccharomyces cerevisiae* (subsequently referred to as "yeast"), homologous recombination is an extremely efficient process, and as such this organism has become the premier eukaryote with which to study mechanisms of homologous recombination (Paques and Haber 1999).

Given the marked propensity for yeast to undergo homologous recombination, the mechanisms and consequences of nonhomologous end joining (NHEJ) have been much less well studied in this organism. End joining has been examined under circumstances in which homologous recombination is not possible due to either lack of homology (Schiestl and Petes 1991; Schiestl *et al.* 1993; Moore and Haber 1996a) or lack of an essential component (*e.g.*, Rad52p) in the homologous recombination pathway (Kramer *et al.* 1994; Schiestl *et al.* 1994). Relying in part on work from mammalian systems, 11 genes associated with NHEJ have been identified: *YKU70* (also known as *HDF1*), *YKU80* (also known as *HDF2*), *DNL4*, *LIF1*, *RAD50*, *MRE11*, *XRS2*, *SIR2*, *SIR3*, and *SIR4* (reviewed by Lewis and Resnick 2000) and most recently *NEJ1* (Frank-Vaillant and Marcand 2001; Kegel *et al.* 2001; Ooi *et al.* 2001; Valencia *et al.* 2001). Several studies have shown that NHEJ is not a homogeneous process but can be divided into a more efficient and error-free simple religation pathway and a less efficient and more error-prone imprecise end-joining pathway (Boulton and Jackson 1996a; Moore and Haber 1996a; Verkaik *et al.* 2002).

In mammalian cells, chromosomal rearrangements can lead to malignant transformation and genetic disorders. Where examined, these rearrangements appear to arise primarily by NHEJ (Woods-Samuels *et al.* 1991; Wiemels and Greaves 1999; Legoix *et al.* 2000; Rothkamm *et al.* 2001). In yeast, spontaneously generated gross chromosomal rearrangements have been observed due to either homologous recombination between multicopy repeat sequences (Codon *et al.* 1997; Casaregola *et al.* 1998; Fischer *et al.* 2000; Umezu *et al.* 2002) or, more rarely (<1 in a billion divisions), other mechanisms involving little or no homology at the breakpoints (Chen *et al.* 1998; Chen and Kolodner 1999). Experimentally derived rearrangements in yeast have generally been based on systems where homologous sequences are placed on the same or different chromosomes, and a DSB is generated by treatment with DNA-damaging agents or endonucleases. Recombination events that sub-

[1]*Corresponding author:* CABM 306, 679 Hoes Lane, Piscataway, NJ 08854. E-mail: gabriel@cabm.rutgers.edu

sequently occur between the two homologous sequences are then selected and scored (Potier *et al.* 1982; Sugawara and Szostak 1983; Fasullo and Davis 1988; Schiestl 1989; Fishman-Lobell *et al.* 1992; Fasullo *et al.* 1994; Haber and Leung 1996).

Relatively little work has focused on the experimental generation of chromosomal rearrangements by NHEJ pathways in yeast following a DSB. Kramer *et al.* (1994) showed that the typical mechanism of repair is rejoining, with gain or loss of very little sequence from the broken ends. In some cases more extensive deletions were seen but these events were not systematically characterized. Moore and Haber (1996a) found that the proportion of these larger deletions was increased by mutations in *MRE11*, *XRS2*, or *RAD50*, or by restricting expression of HO endonuclease to the G_1 phase of the cell cycle. In the only yeast study that has looked for homology-independent chromosomal DSB repair events in the absence of yeast Ku proteins, none were found among 100 potential repair events (Clikeman *et al.* 2001). We and others have found that extrachromosomal DNA sequences, either cDNA or mitochondrial DNA fragments, can become inserted at a DSB in a way that resembles NHEJ (Moore and Haber 1996b; Teng *et al.* 1996; Ricchetti *et al.* 1999; Yu and Gabriel 1999). However, it is unclear how these and other rare rearrangements fit into the broader range of yeast DSB repair events.

We present here an assay designed to select for rare chromosomal rearrangements associated with repair of a DSB in a variety of genetic backgrounds. This assay was previously used to show that Ty1 and mitochondrial fragments could repair a DSB by inserting between the ends, in a process that is *RAD52* independent (Yu and Gabriel 1999). Here, we use this assay to show that the insertion process is *YKU80* dependent. Further, we find that deletions of various lengths, ranging from several bases to several kilobases, can occur in the presence or absence of Yku80p and Rad52p. We observe and characterize a long one-sided type of deletion in all backgrounds that is proportionately more common in cells lacking Yku80p. Smaller deletions, however, are much more dependent on Yku80p. Finally, the assay provides evidence for a *RAD52*-dependent mutagenic form of gene conversion that occurs in the region at the junction between identity and heterology.

MATERIALS AND METHODS

Plasmids and yeast strains: The experiments were carried out using a set of eight isogenic strains, all derived from YFP17 (Δ*hml::ADE1*, Δ*mata::hisG*, Δ*hmr::ADE1*, *ade3::GAL-HO*, *leu2::HOcs*, *ura3-52*; Paques *et al.* 1998). Construction of the *URA3::actin intron* and *URA3::actin intron::HO cut site* cassettes has been previously described (Yu and Gabriel 1999). Likewise construction of strains AGY150 (YFP17, *LEU2, URA3::actin intron* is WT, 0 cut site), AGY117 (YFP17, *URA3::actin intron::HO cut site* is WT, 1 cut site), AGY391 (YFP17, *LEU2, URA3::actin intron,* Δ*rad52::hisG* is *rad52*, 0 cut site), and AGY127 (YFP17, *LEU2, URA3::actin intron::HO cut site,* Δ*rad52::hisG* is *rad52*, 1 cut site) have been described (Yu and Gabriel 1999). In brief, YFP17 was converted to test strains by replacement of *leu2::*HOcs with *LEU2*, and by replacement of *ura3-52* with either *URA3::actin intron* or *URA3::actin intron::HO cut site.*

Strains AGY293 (YFP17, *LEU2, URA3::actin intron,* Δ*yku80::KanMX4* is *yku80*, 0 cut site), AGY287 (YFP17, *LEU2, URA3::actin intron::HO cut site,* Δ*yku80::KanMX4* is *yku80*, 1 cut site), AGY407 (YFP17, *LEU2, URA3::actin intron,* Δ*yku80::KanMX4,* Δ*rad52::hisG* is *rad52 yku80*, 0 cut site) and AGY481 (YFP17, *LEU2, URA3::actin intron::HO cut site,* Δ*yku80::KanMX4,* Δ*rad52::hisG* is *rad52 yku80*, 1 cut site) were constructed as follows: The Δ*yku80::KanMX4* mutation was obtained by one-step disruption (Wach *et al.* 1994). The Δ*yku80::KanMX4* module was amplified with primer RAG484 (5′-TTG AAC TAG TTC AGC AAC CG-3′) and primer RAG485 (5′-AAA AAA GTA GTG CGC GAC AC-3′), using genomic DNA from a yeast strain containing Δ*yku80::KanMX4* constructed by O. Uzun and A. Gabriel (unpublished data). The integrity of the Δ*yku80::KanMX4* sequence was checked with primers RAG634 (5′-CGA CAT CAT CTG CCC AGA TG-3′) and RAG637 (5′-TTC GGG CGG CAG TCA TCC AG-3′). A two-step procedure was used to obtain the Δ*rad52::hisG* mutation (Alani *et al.* 1987). All strains were checked by PCR of the genomic DNA and by Southern blot.

Media and growth conditions: Yeast cells were grown in yeast extract-peptone-dextrose (YPD) or synthetic complete media (SC) with appropriate amino acids missing (Sherman *et al.* 1986). Yeast extract-peptone-galactose (YEP-galactose) and yeast extract-peptone-raffinose (YEP-raffinose) contain 2% galactose (w/v) and 1% raffinose (w/v), respectively, instead of dextrose (2%). 5-Fluoroorotic acid (5-FOA) plates are SC-glucose plates supplemented with 1 mg/ml of 5-FOA (Boeke *et al.* 1984; Sikorski and Boeke 1991).

Induction of HO endonuclease, measurement of DSB repair efficiency (survival frequency), and 5-FOA resistance frequencies: Multiple independent colonies from each strain were grown at 30° in YEP-raffinose liquid medium, to a final concentration of $\sim 3 \times 10^7$ cells/ml, to prepare the cells for galactose induction. Appropriate dilutions of cells were then plated on YPD or YEP-galactose plates. After 4 days of growth, the colonies were counted. Colonies on the YEP-galactose plates were replica plated onto synthetic complete 5-FOA-containing media to measure the frequency of 5-FOA resistance among the survivors of HO endonuclease induction. Survival frequency was calculated as the ratio of the number of colonies growing on YEP-galactose per milliliter of cells plated *vs.* the number of colonies growing on YPD per milliliter of cells plated. The frequency of 5-FOA resistance per survivor was calculated as the ratio of the number of colonies growing on 5-FOA-containing replica plates per milliliter of cells plated divided by the number of colonies growing on YEP-galactose plates per milliliter of cells plated. The absolute frequency of 5-FOA resistance per cell plated was calculated by multiplying together the previous two terms. The absolute frequency of specific types of rearrangements per cell plated was determined for each strain by multiplying the previous calculation by the proportion of the total 5-FOA-resistant colonies shown to have that rearrangement. The proportion of aberrant gene conversions among all gene conversions was determined by dividing the absolute frequency of aberrant gene conversions, based on their proportion among 5-FOA-resistant cells per cell plated, by the absolute frequency of gene conversions, based on their proportion among surviving cells per cell plated.

Analysis of surviving and 5-FOA-resistant colonies: 5-FOA-sensitive or 5-FOA-resistant colonies from the above experiments were single colony purified, patched, and then grown

to saturation in liquid YPD media at 30° before genomic DNA was extracted (Hoffman and Winston 1987). Portions of the *URA3::actin intron::HO cut site* region centered on the HO endonuclease recognition sequence were PCR amplified using *Taq* DNA polymerase. The oligomers used for amplification were RAG512 (5′-GCG AGG CAT ATT TAT GGT GAA GG-3′) and RAG515 (5′-GGA GTT CAA TGC GTC CAT C-3′), both of which are sequences flanking the *URA3* locus. Primers were added to a final concentration of 0.2 μM for each reaction. The PCR consisted of 30 cycles of 30 sec at 92°, 30 sec at 55°, and 1–3 min at 72° in a DNA thermal cycler (Perkin-Elmer, Norwalk, CT). The amplified products were visualized on 0.8% agarose gel and representative samples were sequenced.

Clones that repeatedly failed to amplify using a variety of primers from both sides of the HO cut site, but that did amplify using control primers at other loci, were subjected to inverse PCR to identify junctional sequences. On the basis of these results, appropriate primers were generated for further PCR and sequencing reactions, to clarify the junctions.

To ensure independence of the colonies selected for analysis, 5-FOA-sensitive or 5-FOA-resistant colonies from multiple trials were picked from separate galactose-containing plates whenever possible or from widely spaced regions of the same plate, when necessary. Cells were not exposed to galactose and, therefore, DSB induction until they had been spread on galactose-containing plates. In control experiments, spontaneous 5-FOA-resistant colonies (*i.e.*, those without exposure to galactose) occurred at $<1 \times 10^{-7}$/cell plated, similar to the frequency of 5-FOA resistance on galactose in the absence of an HO cut site. This indicates that leaky HO expression was not a significant source of 5-FOA-resistant cells, prior to induction.

DNA sequencing: PCR products were sequenced according to the dsDNA cycle sequencing technique provided by GIBCO BRL, using [γ-^{32}P]ATP from DuPont NEN Research Products (Boston). The sequencing primers used were RAG513 (5′-ATG TTC TAG CGC TTG CAC CAT C-3′), RAG444 (5′-TGT TAG CGG TTT GAA GCA GG-3′), RAG442 (5′-TTA GTT GAA GCA TTA GGT CC-3′), RAG633 (5′-TTT CAA GCC CCT ATT TAT TCC-3′) for *URA3*. Sequences obtained were identified using BLAST searches of the *Saccharomyces* Genome Database (http://genome-www.stanford.edu/Saccharomyces/).

Inverse PCR: Nonamplifiable genomic DNAs were further analyzed with inverse PCR (Ochman *et al.* 1988) as follows: 5 μg of genomic DNA was digested with *Nsi*I and then circularized by addition of T4 DNA ligase under dilute conditions. The ligated samples were then amplified with pairs of primers, both from the same side of the HO cut site, but oriented away from each other. The primers used for amplification were RAG614 (5′-GTA GAG GGT GAA CGT TAC AG-3′) with RAG445 (5′-TTC TCC AGT AGA TAG GGA GC-3′) and RAG613 (5′-AGC GTC TGC TCT AGC GTT AC-3′) with RAG444. The amplified products of the inverse PCR were then sequenced with primers RAG513 or RAG619 (5′-CAG TCA ATA TAG GAG GTT ATG-3′).

Statistical analysis: Comparisons of deletion lengths and overlap lengths (including 0 overlap) in the presence or absence of *YKU80* were made using the nonparametric Mann-Whitney rank test, with an $N = 11$ for Yku80p present and $N = 27$ for Yku80p absent. Comparisons of survival in different strain backgrounds were made using similar nonparametric tests, with an $N = 20$ for WT, $N = 23$ for *rad52*, $N = 14$ for *yku80*, and $N = 12$ for *rad52 yku80*.

RESULTS

Using a counterselection assay designed to identify insertion events that repair a unique chromosomal DSB in yeast (Yu and Gabriel 1999), we observed a variety of DSB repair events, many involving aspects of chromosomal rearrangements that either have not previously been noted or have not been extensively analyzed in yeast. The basis for this assay (Figure 1A) is a unique HO endonuclease cut site (117 bases of *MAT***a** sequence, spanning the Y/Z junction) placed into a nonessential portion of the actin (*ACT1*) intron, which has itself been engineered into the coding domain of the *URA3* gene on chromosome V. This modified *URA3* allele is fully functional (Yu and Gabriel 1999). When cells are plated on galactose-containing media, HO endonuclease is expressed and a persistent DSB is created at the intronic HO target site. Since the experiments are performed in haploid strains, cells will die unless the DSB is repaired. However, in this strain, error-free repair mechanisms are not available. The *MAT* sequence is unique, so homologous recombination is not an efficient alternative for repair even though sequences homologous to the *ACT1* intron are present at the *ACT1* locus on chromosome VI. Because of the high level of HO endonuclease, both sister chromatids would likely be cut in G_2, eliminating sister chromatid recombination as a viable repair option. If the break is repaired by precise religation, it will be recut by HO endonuclease. Cells must therefore utilize less efficient repair pathways to form HO endonuclease-resistant colonies, including imprecise end joining and gene conversion of the *ACT1* sequences. Because these repair events occur within a nonessential portion of the intron, neither imprecise end joining nor gene conversion should interfere with intron function. Repair of the broken chromosome should leave *URA3* expression unaffected and the cells sensitive to 5-FOA. However, we observed that a fraction of survivors become uracil auxotrophs (*i.e.*, 5-FOA resistant), because of repair events associated with more complex chromosomal rearrangements. The frequency and spectrum of surviving uracil auxotrophs and prototrophs depended on the specific genetic background of the yeast strain.

Survival after a DSB: To characterize the variety of DSB repair events observable with our system, we analyzed survivors that had either retained or lost *URA3* function after receiving a DSB in the presence or absence of Rad52p or Yku80p. As shown in Figure 1B, expression of HO endonuclease in the absence of an HO cut site sequence within the *URA3::actin intron* had little effect on cell survival (77–94% survival for all four 0 cut site strains). In the presence of the unique HO cut site, only 1.9% of the WT cells survived persistent expression of HO endonuclease, a 48-fold decrease compared to the 0 cut site strain. In the absence of *RAD52*, 0.45% of cells survived expression of HO endonuclease, a 208-fold decrease compared to the 0 cut site control and a >4-fold decrease compared to WT ($P < 0.001$). This suggests that repair events mediated through Rad52p play a role in the survival of cells after

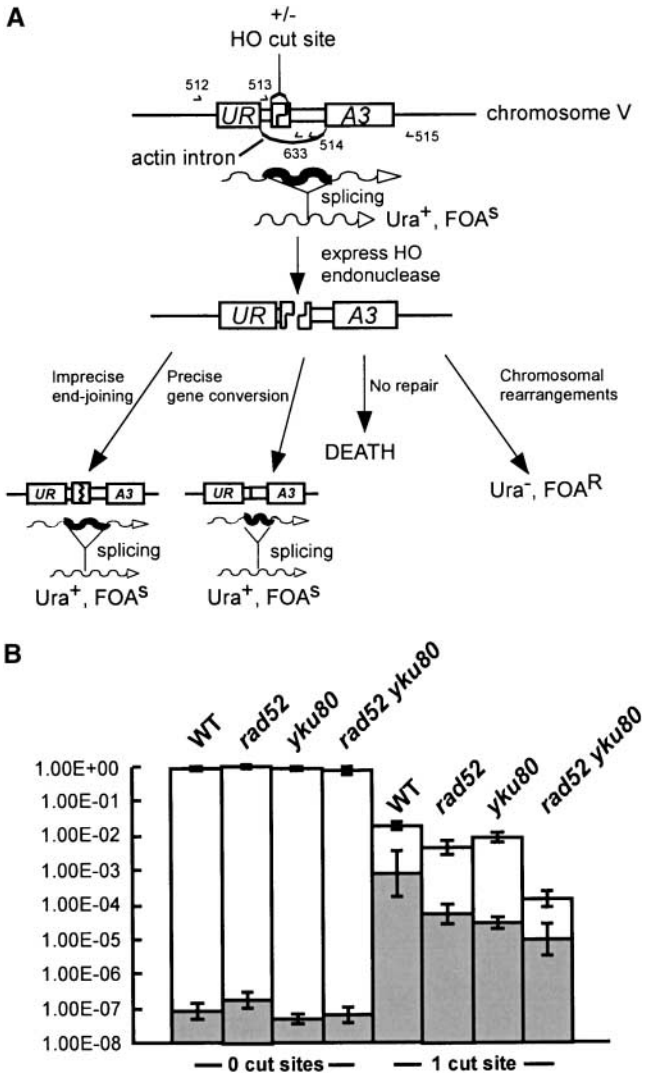

FIGURE 1.—The *URA3::actin intron* assay system. (A) Structure of the *URA3::actin intron* allele on *S. cerevisiae* chromosome V, used in this study. The presence or absence of the 117-bp HO recognition sequence (*i.e.*, HO cut site), distinguishes 1 cut site from 0 cut site strains. The approximate positions of various oligonucleotide primers (numbers and carets) used for PCR and sequencing are shown (as described in MATERIALS AND METHODS). The *ACT1* intron placed into the *URA3* gene is normally spliced, resulting in uracil prototrophy (Ura^+) and sensitivity to the drug 5-fluoroorotic acid ($5\text{-}FOA^S$). After creating a persistent DSB with HO endonuclease, a proportion of cells have a DSB that cannot be repaired and do not survive. Other cells are repaired by simple imprecise end joining or precise gene conversion, which allows for normal splicing. Still other cells are repaired in ways that result in chromosomal rearrangements, which directly or indirectly prevent splicing. The latter situation leads to a phenotype of uracil auxotrophy (Ura^-) and resistance to 5-FOA ($5\text{-}FOA^R$). (B) Comparison of frequencies of survival and 5-FOA resistance. Bars represent the frequencies per plated cell. Open bars represent mean survival frequencies and shaded bars represent 5-FOA resistance among plated cells. Frequencies are plotted on a log scale. Standard deviations are shown as error bars. Each mean survival frequency was based on between 12 and 23 independent trials, involving a minimum of three separate experiments.

a DSB. Elimination of Yku80p instead of Rad52p had a similar negative effect on survival, with only 0.84% of cells surviving ($P < 0.001$, compared to WT, and $P < 0.005$ compared to *rad52* cells). When both genes were absent, survival after a DSB was much less common, with a frequency of only 0.015%, nearly 5200-fold decreased compared to that of the 0 cut site control and >100-fold lower than that of the equivalently cut WT strain ($P < 0.001$ compared to WT, and $P < 0.002$ compared to *rad52* or *yku80*). Thus, while overall survival after a DSB is impaired in our assay system, it is maintained at a low level by a combination of inefficient homologous and nonhomologous repair pathways. The presence of either Rad52p or Yku80p allows cells to survive at levels ~2- to 4-fold below WT. These pathways appear to function independently, since in the absence of both proteins, survival after a DSB is reduced >100-fold, to ~1 in 10,000 cells.

To determine the basis for survival in these different genetic backgrounds, we PCR amplified the region surrounding the engineered *actin intron::HO cut site* in surviving colonies (Figure 2). Two classes were observed. The first class contained PCR products that were close to parental length while the second class was ~130 bp shorter than the control parental PCR product. Sequence analysis of representative samples of both classes clarified their origins. The larger PCR products contained 0–6 base deletions or 0–4 base insertions, corresponding to imprecise nonhomologous end joining of the HO cut site, with resulting loss of the HO recognition sequence. Similar repair products have been previously reported after persistent HO-induced DSBs (KRAMER *et al.* 1994; MOORE and HABER 1996a; CLIKEMAN *et al.* 2001). The smaller PCR products contained the precise sequence of the *ACT1* intron, with the entire engineered HO cut site eliminated. This likely occurred by homologous recombination, *i.e.*, DSB-stimulated gene conversion of the *URA3::actin intron* site by the endogenous *ACT1* intron, despite the region of terminal nonhomology flanking the cut site (48 bases of *MAT* sequence on one side of the HO cut and 69 bases on the other side; PAQUES and HABER 1997).

Among 37 WT survivors we observed both classes of survivors, with those derived from imprecise end joining (43%) being almost as frequent as those derived from gene conversion (57%). In the absence of *RAD52*, all 14 survivors examined by PCR were approximately of parental size, and 12/14 sequenced products showed imprecise rejoining. The remaining 2 had no apparent change around the HO cut site. All 37 PCR products from the *yku80* strain were ~130 bp shorter than the parent and sequencing revealed precise elimination of the inserted HO target site region in 4/4 products. We also sequenced 20 of the DSB survivors in the strain deleted for both *RAD52* and *YKU80*. In each case the PCR product was of parental size, and there was no apparent change in the *MAT* sequence, suggesting that cutting had not occurred. Given that these surviving

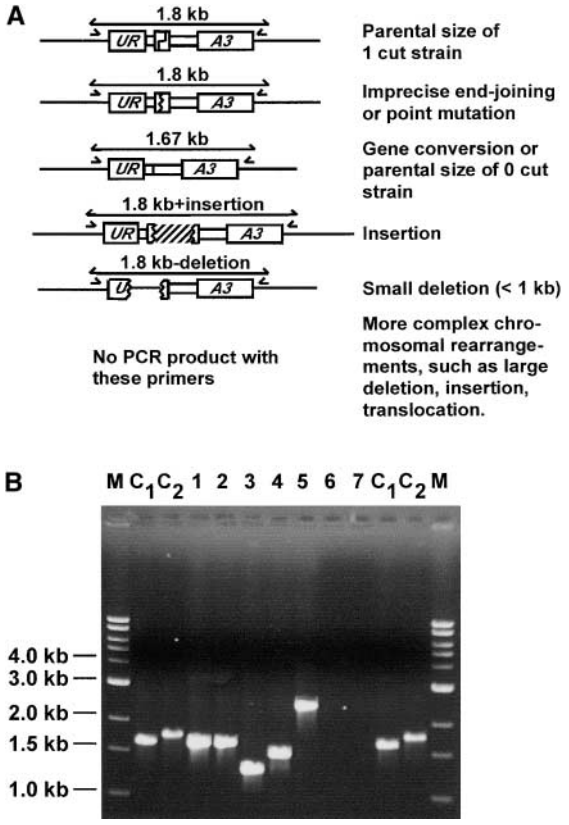

FIGURE 2.—PCR analysis of 5-FOA-sensitive and 5-FOA-resistant survivors exposed to HO endonuclease. (A) Predicted sizes of different PCR products using primers RAG512 and RAG515. (B) PCR amplification around the HO cut site of cells that have repaired the HO cut, corresponding to the following genomic DNA samples and using the primer pair in A: (1) y1701 (aberrant gene conversion), (2) y1703 (aberrant gene conversion), (3) y1444 (deletion of 495 bp), (4) y1496 (deletion of 298 bp), (5) y1497 (insertion of Ty1 656 bp), (6) y1365 (later determined to be a 5.3-kb deletion), and (7) y1424 (later determined to be a translocation). C1 and C2 refer to the products for the *URA3::actin intron* and *URA3::actin intron::HO cut site* parents, respectively. M refers to the 1-kb DNA ladder (New England Biolabs, Beverly, MA).

cells grew up at a frequency ~100-fold lower than that of the induced WT cells, it is most likely that *rad52 yku80* survivors represent the background of rare cells that either have not been induced or have become resistant to cutting, through either genetic or epigenetic changes.

Chromosomal rearrangements among survivors of a DSB: We next characterized the loss of *URA3* expression (*i.e.*, 5-FOA resistance) among survivors of a persistent DSB; 5-FOA resistance in control strains lacking the HO recognition sequence is exceedingly rare ($<1 \times 10^{-7}$/survivor) regardless of the background (Figure 1B). In all cases examined ($N = 78$), PCR products from the *URA3* locus were of parental size, suggesting that point mutations within the *URA3* gene were the most common source of spontaneous 5-FOA resistance.

In response to an induced DSB, the frequency of 5-FOA resistance per plated WT cell increased nearly 10,000 fold, indicating that a persistent DSB predisposes a cell to error-prone repair. However, in all strains tested, the 5-FOA-resistant cells were a small minority of the total survivors, ranging from 0.47% (*yku80*) to 6.40% (*rad52 yku80*). We used PCR to assess changes at the *URA3* locus. As shown in Figure 2, we could distinguish several patterns of PCR products, including parental size, 130 bp shorter than the parent, other shorter products, and larger products, as well as no products detected. Using a variety of techniques (see MATERIALS AND METHODS), we determined the types of rearrangement resulting in 5-FOA resistance for a large number of independent colonies in each of the four backgrounds. As shown in Table 1, the proportion of each type of 5-FOA-resistant rearrangement varied by the genetic background. From these data we could estimate the absolute frequency of each type of rearrangement among cells exposed to a persistent DSB. The widest range of rearrangements occurred in WT cells. This spectrum was narrowed in the single mutant strains, and in the double mutant strain we could detect only deletions. Below, we report on the nature of the different chromosomal rearrangements associated with DSB repair in different genetic backgrounds.

Deletions: Although we observed deletions in all strain backgrounds (Table 1; Figures 3 and 4), their frequency and the extent of deleted sequence was strain dependent. We divided deletions into smaller (>117 bp but <1 kb, Figure 3) and larger (>1 kb, Figure 4). Deletions of <117 bp, involving only the HO cut site sequence and nonessential portions of the intron, do not interfere with *URA3* expression and go undetected. The smaller deletions were within *URA3*, and therefore identifiable by our screening PCR procedure. Larger deletions initially gave no PCR products, but were identified by inverse PCR. Deletion lengths were also restricted by the location of flanking essential genes. In the telomeric direction from *URA3*, the first essential gene is *SNU13*, 14 kb away. In the centromeric direction, the very next open reading frame (ORF), *TIM9* (930 bp from the cut site), is essential.

In WT cells, deletions accounted for <10% of all 5-FOA-resistant colonies (absolute frequency of 7×10^{-5}/plated cell). Of the four independent events sequenced, three (y1496, y190, and y781) were <1 kb. In two cases, two or five identical bases present in the parental chromosome on both sides of the cut site were found overlapping at the deletion junction. We refer to this as "overlapping microhomology." No overlap was present at the third junction (Figure 3). The fourth deletion (y774) was missing 5.3 kb of sequence including the 5′ half of *URA3* and the flanking nonessential gene *GEA2* (Figure 4). This event was noteworthy for several reasons. The deletion junction consists of an 11/12 base overlap, which is larger than the typically observed 0- to 6-bp microhomology in yeast NHEJ (SCHIESTL *et al.* 1993; KRAMER *et al.* 1994; MOORE and HABER 1996a). The

TABLE 1

Repair and rearrangements after a DSB at the *URA3::actin intron::HO cut site* locus

Genetic background	Frequency of survival per plated cell	Frequency of 5-FOA resistance per plated cell	Chromosomal rearrangements resulting in 5-FOA resistance						
			Insertions (%)	Gene conversions (%)	Small deletions[a] (%)	Large deletions[b] (%)	Translocations and inversions (%)	Unknown[c] (%)	N[d]
WT	1.90×10^{-2}	7.51×10^{-4}	40	4	7	2	17	30	46
rad52	4.51×10^{-3}	5.83×10^{-5}	52		19	5	12	12	42
yku80	8.39×10^{-3}	3.61×10^{-5}		78	1	21			150
rad52 yku80	1.49×10^{-4}	1.05×10^{-5}			5	87		8	79

[a] Small deletions are between 117 and 1000 bp.
[b] Large deletions are >1 kb.
[c] The unknown events are the 5-FOA-resistant clones for which no PCR product was obtained using all means described (WT, *rad52*, and *rad52 yku80*).
[d] *N* refers to the nos. of independent 5-FOA-resistant colonies from which genomic DNA was obtained and analyzed.

deletion is distinctly asymmetric, with >5 kb missing from one side of the HO cut, but only the four overhanging 3′ bases, AACA, deleted from the other side of the HO cut site. Finally, this same deletion was independently observed in all strain backgrounds (see below) and, in the mutant backgrounds, occurred at approximately the same absolute frequency (*i.e.*, 3–5 $\times$ 10^{-6}/plated cell).

For *rad52* cells, smaller deletions accounted for 19% of all 5-FOA-resistant clones (absolute frequency of 1 $\times$ 10^{-5}/plated cell). We sequenced five smaller deletions (y1443, y793, y1444, y1421, and y1427) and found they were similar to the WT deletions. The average deletion length was ~300 bp in both WT and *rad52* strains. Overlapping microhomology was present in each case (4, 3, 6/7, and two 8/9 bp; Figure 3). In addition, we identified two independent larger deletions (y1434 and y1440) in this background (4.8% of all 5-FOA-resistant colonies, absolute frequency of 3 $\times$ 10^{-6}/plated cell). They were both identical to the 5.3-kb deletion observed in WT cells. The pattern of deletions for WT and *rad52* cells was quite similar, suggesting that Rad52p is not directly involved in deletion formation.

In *yku80* cells, deletions accounted for ~22% of the 5-FOA-resistant clones (absolute frequency of 8 $\times$ 10^{-6}/plated cell) but only two of eight deletions sequenced were <1 kb (235- and 934-bp deletion lengths; Figure 3). One clone (y1368) had extensive sequence loss on both sides of the HO cut site, with an 18-/22-bp overlapping junction. The other (y2177) had a 5-base overlap. The remaining deletions were all >1 kb. Four of these (y715, y761, y1365, and y1375; Figure 4) were the same 5.3-kb deletion observed in the WT and *rad52* backgrounds. The other two (y755 and y730) were even larger deletions, extending 9.3 and 12.9 kb toward the telomere, eliminating three other nonessential genes (*YEL025C*, *RIP1*, and *YEL023C*). These two deletions had overlaps of 9/10 bases and 7/ 8 bases, respectively.

In *rad52 yku80* cells, 92.4% of the total 5-FOA-resistant colonies clearly resulted from deletions (absolute frequency of 1 $\times$ 10^{-5}/plated cell), of which only 5.1% were <1 kb in length. Of 4 smaller deletions sequenced, 2 (y1969 and y2001) extended on both sides of the HO cut site for 406 and 436 bp and overlapped by 16/20 and 14/16 bp, respectively. The other 2 (y1963 and y1997) were deleted primarily on one side of the cut site, by 551 and 741 bp and had overlaps of 7/7 and 6/6 bases (Figure 3). We obtained sequence data from 16 of the larger deletions. The 5.3-kb deletion observed in the other backgrounds was identified in seven independent clones (y1971, y1972, y1979, y1981, y1982, y1984, and y1987). Additionally, a wide array of long one-sided deletions was seen, ranging from 2.1 to 12.2 kb (y1973, y1975, y1968, y1978, y1983, y1976, y1970, y1985, and y1989). These deletions were similar to those in the *yku80* strain background, again suggesting that Rad52p did not play a significant role in the formation of these rearrangements. Further, the relative shift from smaller to larger deletions in the *yku80* and *rad52 yku80* strains suggested that one role for Yku80p is to limit the extent of DNA digestion after a DSB.

We carried out a statistical analysis of all deletions in the absence or presence of Yku80p. Deletion lengths in the absence of Yku80p were significantly greater than those in the presence of Yku80p ($P < 0.002$), averaging 5900 and 1700 bp, respectively. Differences in the length of overlap at the junctions were also statistically significant ($P < 0.005$), with averages of 11.2 and 6.6 bp, respectively. These findings suggest that different mechanisms of deletion formation predominate in the presence or absence of Yku80p.

Aberrant gene conversions: In both WT and *yku80* strains, we identified a distinct class of 5-FOA-resistant amplification products that were ~130 bp shorter than the parent (absolute frequency of ~3 $\times$ 10^{-5}/plated cell, for each strain). These products were not observed in *rad52* or *rad52 ku80* cells, which are incapable of homologous recombination (Table 1). In the case of 5-FOA-

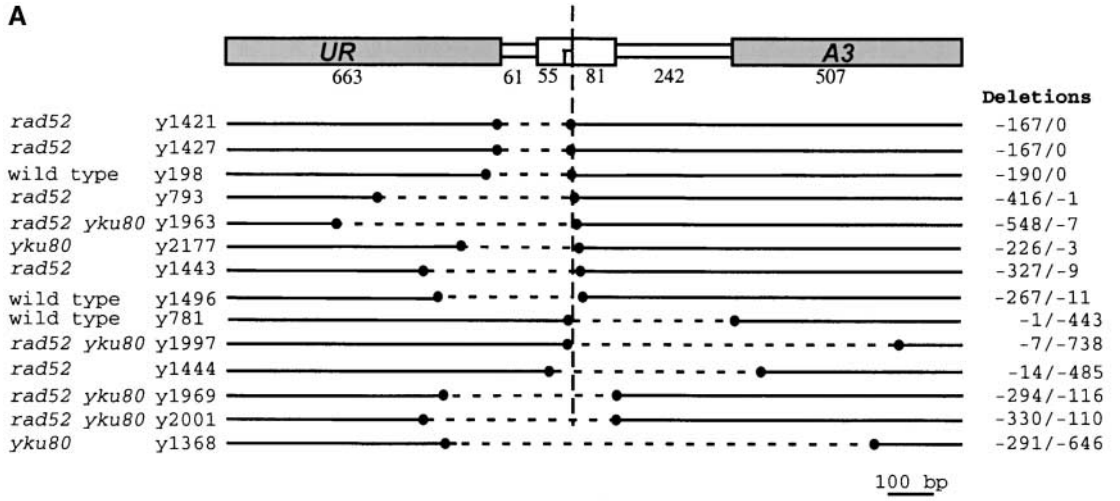

B

Overlap/segment

```
HO cut site:    AAAACCAGGGTTTATAAAATTATACTGTT_________TGTTGCGGAAAGCTGAAACTAAAAGAAAAA

y1421, y1427    GGGCCCAGGTAT(tgttagcggttt.....)TGTTGCGGAAAGCTGAAACTAAAAGAAAAA  8/9
    y198        GGGCAGACATTACGAA(tgcac.....)TGTTGCGGAAAGCTGAAACTAAAAGAAAAA  2/2
    y793        AAGGAATTACTGGA(gttagt.....t)GTTGCGGAAAGCTGAAACTAAAAGAAAAA  3/3
    y1963       GATAAATCATGTC(gaaagctaca.....gcg)GAAAGCTGAAACTAAAAGAAAAA  7/7
    y2177       GCAGTACTC(tgcgggtg.....tgt)TGCGGAAAGCTGAAACTAAAAGAAAAA  5/5
    y1443       GCACAGTT(aagccgc.....gga)AAGCTGAAACTAAAAGAAAAA  4/4
    y1496       CAGAAAATTT(gctgacattg.....aaa)GCTGAAACTAAAAGAAAAA  5/5

    y781        AAAACCAGGGTTTATAAAATTATACTGT(t.....aga)GGACATGGGTGGAAGAG  0/0
    y1997       AAAACCAGGGTTTATAAAATTA(tac.....cacaaatta)GAGCTTCAATTT  6/6
    y1444       AAAACCAGGGTTTAT(aaa.....attggttgat)TATGACACCCGGTGTGG  6/7

    y1969       TCCGCCAAGTACAATTTTT(tactcttcgaaga.....ttttactattttt)CACTCTCCCATA 16/20
    y2001       CCGCCAAGTACA(atttttttactcttcg.....ttttact)ATTTTTCACTCTCCCATA 14/16
    y1368       TGCGGGTGTATACAGAA(tagcagaatgggcagaca....cgttacagaa)AAGCAGGCTGGGAAGCA 18/22
```

FIGURE 3.—Deletions <1 kb are observed in all strain backgrounds. (A) The *URA3::actin intron::HO cut site* cassette with the size of each part labeled. Deletions were sorted by size. Solid lines denote chromosomal sequences and dashed lines denote deletions. The deletion ends are shown as solid dots. The vertical dashed line corresponds to the position of the HO cut site. The left columns indicate strain backgrounds and clone numbers. The right column indicates the extent of the deletions on either side of the cut site (separated by a slash). (B) The specific joint sequence for each deletion is shown in uppercase. The undeleted HO cut site sequence is aligned above all of the individual deletions, with the 4-bp (TGTT) 3′ overhang shown twice. Overlapping bases are underlined. The deletions are shown in parentheses. Overlap/segment indicates the number of identical bases among the junctional sequences. In cases of imperfect overlap, only mismatches with several matching bases on either side were considered, and insertion or deletion mismatches were not considered.

sensitive cells, we found that similarly sized products represented gene conversions where the HO target site had been precisely eliminated and the intact *ACT1* intron had been restored. Therefore, it was of interest to determine how some subpopulation of these gene conversion events could have resulted in loss of *URA3* function.

We sequenced the *URA3::actin intron* region from 9 5-FOA-resistant clones in the WT strain and 23 clones from the *yku80* strain, which had PCR products ~130 bp shorter than the parental band. As shown in Figure 5, in these clones the *ACT1* intron was intact but the sequence upstream of the *ACT1* splice donor (*i.e.*, to the left of the boxed "gt") consisted of 10–15 contiguous bases of *ACT1* exon rather than the expected *URA3* sequence. In one case the length of *ACT1* exon sequence present at the *URA3* locus extended for an additional 4 bases. Upstream of the *ACT1* exon sequence, intact *URA3* sequences were present. Thus, a segment of *URA3* sequence has been replaced by *ACT1* exon sequence. This results in a frameshift; although the intron is intact and can be correctly spliced, the resulting *URA3* ORF is frameshifted just upstream of the site of the intron and is consequently nonfunctional.

Comparison of the sequence of *URA3* and *ACT1* in the region of the altered sequence revealed a segment of fortuitous similarity just upstream of the intron. As shown in Figure 5, 15 of 23 bases are identical for both genes, with four regions of mismatch. This finding suggests that during the homologous recombination event that leads to gene conversion, sequences within the similar segment, physically located between complete homology and complete heterology, are sometimes not precisely distinguished by the repair machinery and are

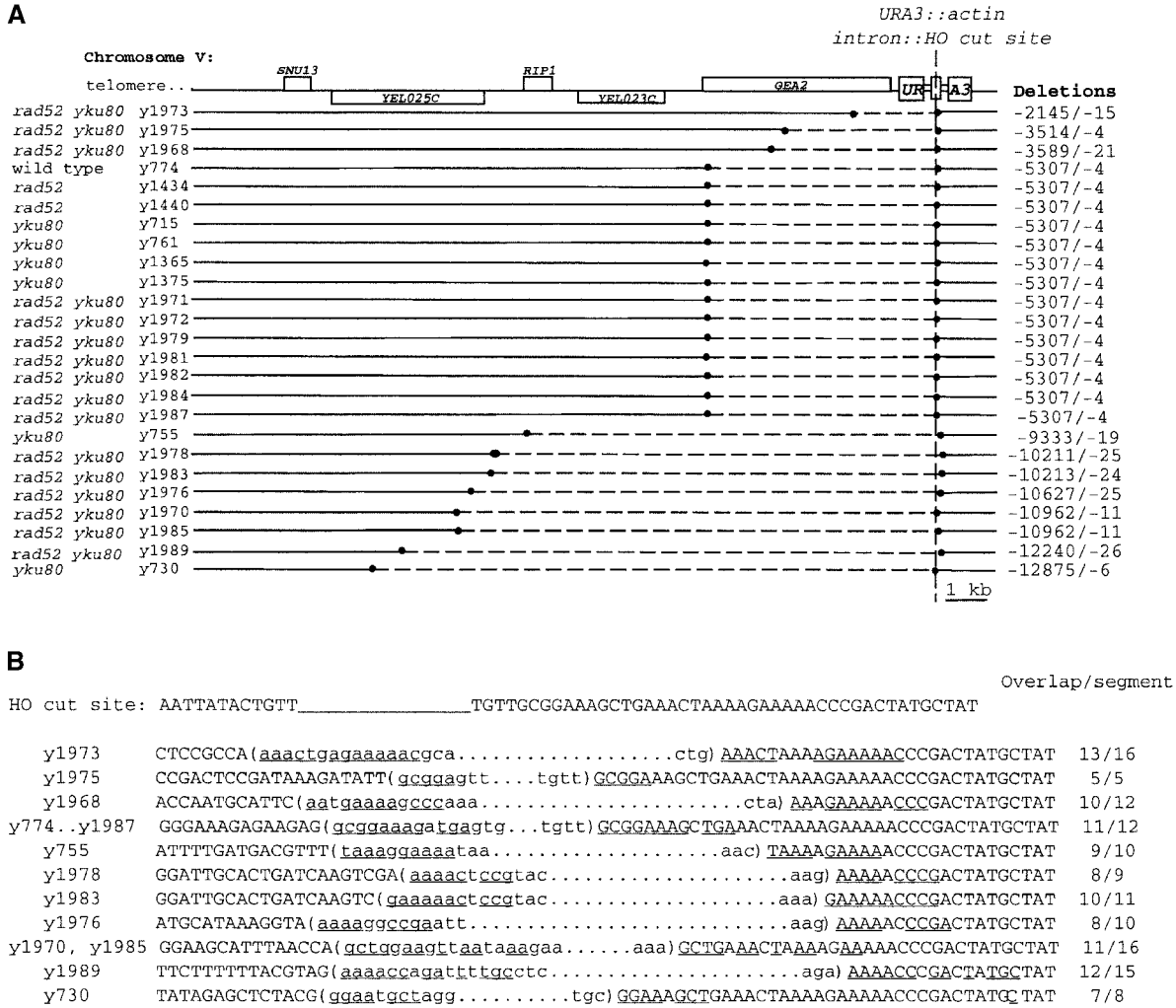

FIGURE 4.—Deletions >1 kb are observed in all strain backgrounds. Several nonessential ORFs are found telomere proximal to the *URA3* gene on chromosome V until the essential gene *SNU13*. The extent of observed large deletions shows which ORFs are lost. Labeling is as in Figure 3.

therefore aberrantly resolved. It is unlikely that Yku80p plays any role in this process, since we estimate that aberrant events account for 0.31% of all gene conversions in WT cells and 0.34% of all gene conversions in *yku80* cells.

Insertions: We previously reported using this assay system to find insertions of both Ty1 (140 bp to 3.4 kb) and mitochondrial DNA sequences (33–219 bp; YU and GABRIEL 1999). Nearly all of the Ty1 insertions joined the break to one of the Ty1 LTR termini and were made up of either continuous or discontinuous stretches of Ty1. In both WT and *rad52* cells, the junctional sequences contained microhomologies, suggestive of NHEJ events. In our current analysis of inverse PCR products, we have identified several large Ty1 insertions. The largest is ~5.6 kb, consisting of a nearly full-length Ty1 element (data not shown).

Since Yku80p is thought to be an essential component of the NHEJ machinery, we examined ~150 independent 5-FOA-resistant *yku80* clones. In no instance did we recover any insertion event (Table 1). Similarly we observed no insertions in 79 independent 5-FOA-resistant *rad52 yku80* clones (Table 1). While it is formally possible that in these strain backgrounds we are missing small insertions that do not result in 5-FOA resistance or very large insertions that we cannot amplify, it appears that insertion of extrachromosomal DNA into a DSB site, as seen in WT and *rad52* cells, either requires or is greatly facilitated by the presence of *YKU80*.

Other events: A subset of 5-FOA-resistant clones from each strain were not amplifiable using PCR primers on either side of the HO cut site in *URA3*. We characterized a large number of such events by inverse PCR and later with additional direct PCR primers (see MATERIALS AND METHODS). One class of these products was translocations and inversions, and these will be analyzed in detail in a separate article. In summary though, most of these rearrangements resulted in joining the broken ends of the *URA3*::*actin intron* locus with chromosomal segments that appear to have suffered concomitant cleavage.

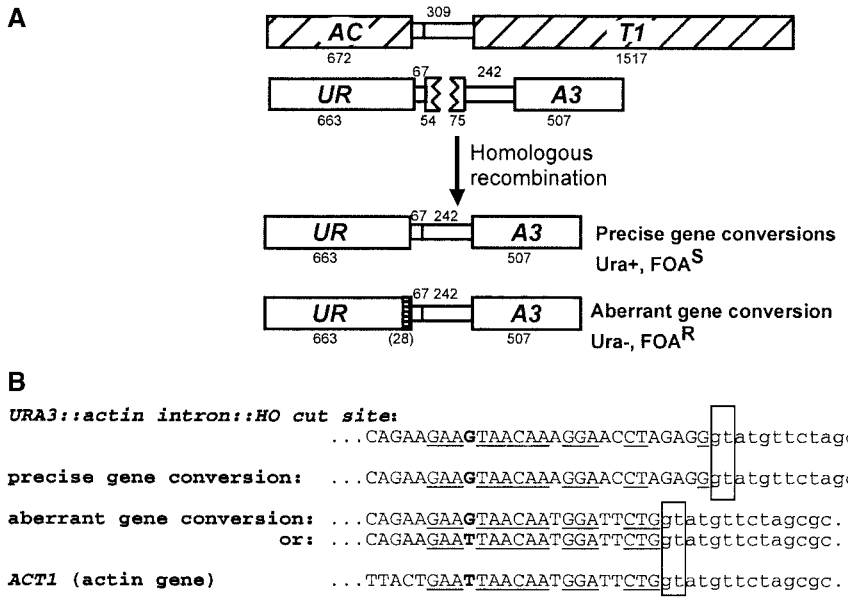

FIGURE 5.—Aberrant gene conversions induced by a DSB at *URA3*. Gene conversion occurs between the *ACT1* intron sequence in the *URA3::actin intron::HO cut site* cassette and the intact endogenous *ACT1* gene. (A) The coding regions of the two genes are shown as wide boxes. The narrow lines represent the *ACT1* intron. The HO cut site is depicted as a wide broken rectangle. The length of each portion is shown. Precise gene conversion results in elimination of the HO cut site sequence from the *ACT1* intron in the *URA3* allele. Aberrant gene conversion additionally results in a small segment of contiguous *ACT1* exon sequence replacing a portion of the *URA3* coding region upstream of the intron splice site (shown as a hatched box within the 5′ half of the *URA3* ORF). (B) The similar but nonidentical sequences involved in this gene conversion. The sequences of *URA3* and the *ACT1* exon are uppercase, while the *ACT1* intron is lowercase. Identical bases within the 19- to 23-base fortuitously similar but nonidentical sequence in *URA3* and *ACT1*, just upstream of the intron, are underlined. Bases "gt" in boxes are the 5′ splice site of the intron. Numbers in parentheses indicate the proportions of observed events.

These gross chromosomal rearrangements after a single DSB were observed in both WT and *rad52* strains and showed typical microhomology between the joined sequences. They were not seen in either the *yku80* or the *rad52 yku80* strain, suggesting that their appearance was strongly dependent on the presence of the NHEJ machinery (Table 1). Other nonamplifiable products could represent very large deletions, deletions with insertions into other parts of the genome, or very large insertions. Further genomic analysis will be required to completely characterize these remaining events.

DISCUSSION

Here we have examined the spectrum of chromosomal rearrangements used by *S. cerevisiae* to repair a DSB in the presence or absence of key components of the homologous recombination and NHEJ pathways. In addition to imprecise end-joining events that have previously been examined in the presence of a persistent HO-induced DSB, we have observed extrachromosomal DNA insertions, deletions of various length, and aberrant gene conversions and noted their dependence on specific repair proteins. Many of the observed rearrangements appear to be mistakes in the context of more straightforward repair pathways. For example, 8 of the 11 deletions we sequenced in WT and *rad52* cells are <1 kb and have junctions similar to the simple imprecise end joins previously reported (KRAMER *et al.* 1994; MOORE and HABER 1996a), except for the increased length of sequence resection (Figure 3). This type of deletion was most often seen in the presence of *YKU80*. Similarly, aberrant gene conversions, only subtly different from normal gene conversions, appear to occur because of an error in discriminating a similar but nonidentical sequence stretch (Figure 5). The existence of such mistakes provides a window on the limitations of the common repair pathways.

Ku-independent deletion formation: An unexpected observation is that Ku-independent deletions appear to represent a distinct repair pathway. We identified a specific 5.3-kb deletion independently and repeatedly in all backgrounds and found that the absolute frequency of this and other long one-sided deletions was similar in the absence or presence of Yku80p ($0.7–1.6 \times 10^{-5}$ events/plated cell). Thus, while these events do occur in the presence of Yku80, they are masked by the higher frequency of other more efficient repair pathways.

Clues to the mechanism of this deletion pathway come from a detailed analysis of the observed events. Extensive sequence elimination is restricted to the telomeric side of the cut, while the sequence of the centromeric side of the break is essentially intact (Figure 4). This asymmetry is reminiscent of previously observed one-sided invasion events during homologous recombination at DSBs (BELMAAZA and CHARTRAND 1994) or of break-induced recombination (KRAUS *et al.* 2001), although the homology thought to drive those events is lacking. While the absence of sequence elimination on the centromeric side may be related to the proximity of the next essential gene ~900 bp from the HO cut site, this does not fit the observed data. With smaller deletions, we observed several 100- to 700-bp deletions toward the centromere, indicating that deletions toward

the centromere can and do occur. However, in no case of a long one-sided deletion were there >26 bases missing on the centromeric side of the cut. This suggests that during Ku-independent deletion formation, one or both strands on the centromeric side of the break are protected from degradation.

The sequence overlaps at the deletion junctions tend to be imperfect. With a mean length of 11.2 bp, they are longer than the typical microhomologies of NHEJ (0–6 bp) but shorter than the ~30 bp thought to be required to support *RAD52*-dependent homologous recombination (Manivasakam *et al.* 1995). This suggests that in the absence of Ku or significant terminal homology, joint formation is difficult and might occur only if the two strands can anneal with sufficient extended complementarity to stabilize the initial joint. To examine this further, we used the first 22 bases from the centromere-proximal side of the cut site as a query sequence and searched for homology in the 10 kb of chromosome V sequence telomeric to the *URA3* locus. The common 5.3-kb deletion junction, containing 11 of 12 bases of homology, was the nearest sequence to the HO cut site with substantial homology and without deletions or insertions.

A working model for Ku-independent deletion formation is shown in Figure 6. After a DSB (Figure 6A), damage can be recognized and acted on by a large number of proteins or protein complexes (Figure 6B). Although we tend to categorize these proteins into separate *RAD52* or NHEJ epistasis groups, some of the proteins or classes of proteins (*e.g.*, the Rad50/Mre11/Xrs2 complex, nucleases, polymerases) likely function in both pathways. In yeast, DSBs are followed by 5′ to 3′ digestion around the break site, leading to exposed 3′ single strands (Haber 1995). We propose that a protein complex, not including Yku80p or Rad52p, binds to one side of the DSB (in this case, the centromeric side), resulting in end protection of one or both strands (Figure 6C). It is conceivable that HO endonuclease remains bound and plays a role in end protection. The resulting complex directs the terminal 3′ sequences on a local complementarity search, beginning from the opposing end of the DSB and perhaps accompanied by a 5′ to 3′ nuclease or a helicase to expose single-stranded regions (Figure 6D). Rad59p, a homolog of Rad52p important for single-strand annealing of short homologous sequences may be involved in this step (Sugawara *et al.* 2000; Davis and Symington 2001). The extent of slower terminal 3′ deletion that occurs on the centromeric side before the protein complex has bound could determine the specific sequences that take part in the complementarity search. Once sufficient complementarity is established and annealing occurs (Figure 6E), the activities of the complex could change (Figure 6F), leading to cleavage of noncomplementary regions, resynthesis of second strands, and finally religation (Figure 6G). Of interest, in all cases of imperfect complementarity shown in Figure 4, the observed sequence at the mismatched positions corresponds to the base present on the centromeric side of the break. This strong bias implies either a directionality of heteroduplex mismatch correction or, alternatively, that after joint formation, resynthesis proceeds first from the searching strand toward the telomere (Figure 6F). The complementary strand would be subsequently processed by removal of the nonhomologous tail, including the mismatch, followed by resynthesis of that strand.

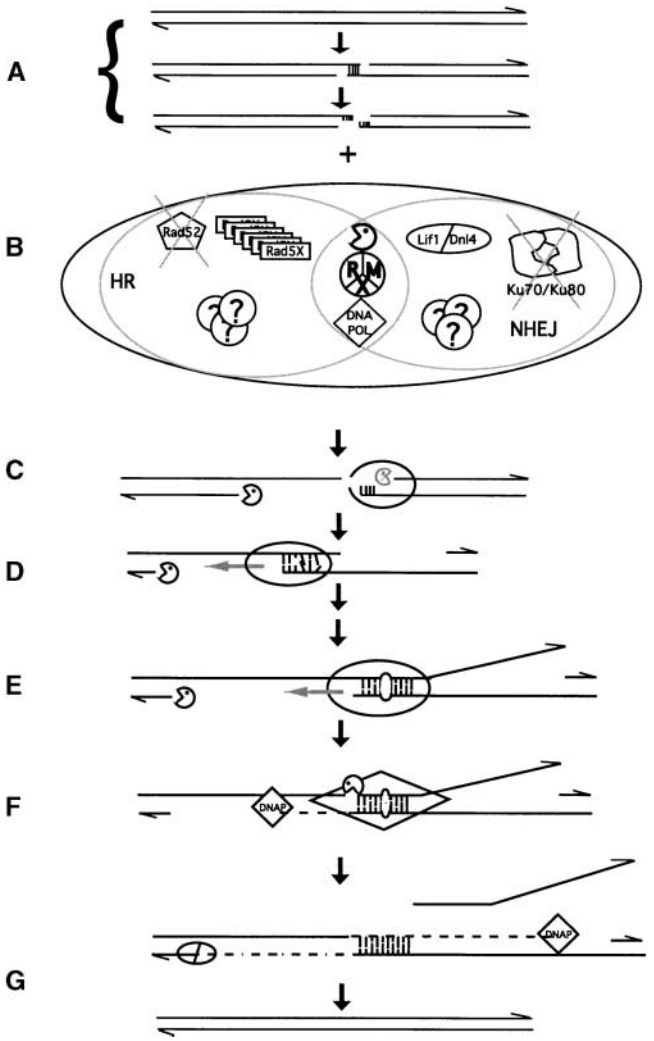

Figure 6.—A model to account for the observed *YKU80*- and *RAD52*-independent long one-sided deletions. Details of the model are presented in the text. Pacman figures represent nucleases. The ellipse in B represents the sum of DSB repair proteins, subdivided into overlapping homologous recombination and nonhomologous end-joining components. The series of Rad5X boxes represents the members of the *RAD52*-epistasis group. The circles with question marks signify that additional unknown proteins may be involved in these processes. The R/M/X circle represents the Rad50/Mre11/Xrs2 complex.

Our system allowed us to generate sufficient numbers of repair events to quantitate and characterize Ku-independent chromosomal deletions, and thereby formu-

late a model for the pathway. A review of the literature indicates older observations consistent with certain aspects of this pathway. In Ku-deficient mammalian cells, excessive DNA degradation has been observed in cells surviving attempted V(D)J rejoining or repair of other DSBs (Schuler *et al.* 1986; Hendrickson *et al.* 1988; Taccioli *et al.* 1993; Liang and Jasin 1996), but the deletion junctions have not been extensively examined. In yeast, Welcker *et al.* (2000) identified spontaneous large deletions in WT and *rad52* strains that contained long imprecise overlapping junctions. Neither the initiating events nor the genetic requirements for these events are known. Similarly, Myung *et al.* (2001) identified spontaneous translocations and deletions involving long imprecisely overlapping sequences at the junctions, in the absence of either Sgs1p or Top3p. In experimental yeast DSB repair systems, Kramer *et al.* (1994) noted that the junctional sequences of several *RAD52*-independent deletions (formed upon rejoining of a ruptured conditionally dicentric chromosome) contained imperfect complementarity, including two with identical 11-/13-bp overlaps. These events occurred in Yku80$^+$ cells after an unusual mitotic breakage event. Mezard and Nicolas (1994) observed similar nonhomologous rejoining events for linearized plasmids transformed into *RAD52* and *rad52* cells. In some cases there was end-to-end joining, but in others joints were either internal-to-internal or internal-to-end (*i.e.*, two- or one-sided deletions). Boulton and Jackson (1996a,b) analyzed the structure of rejoined *Eco*RI linearized plasmids transformed into WT, *yku80*, or *yku70* strains. In WT cells they recovered only precisely rejoined plasmids, but in mutant cells they observed a variety of plasmid deletions ranging from 6 to 811 bp in length, with junctional overlapping sequences of 3–15 bp. They did not observe imprecise end joining in WT cells. Their work suggests that precise rejoining is Ku dependent and demonstrates that deletions are observable when Ku is absent. It does not, however, address whether such deletions still occur in WT cells, but are masked by the higher frequency of precise events. Finally, Moore and Haber (1996a) examined chromosomal HO-induced DSB repair in the absence of homologous recombination in a variety of genetic settings. Although they did not examine Ku mutants, they did recover >700-bp deletions with microhomology at the junctions when they expressed HO continuously in the absence of *RAD50*. When HO was expressed only in G_1, deletions of >700 bp were also seen and were the predominant product in *rad50* cells. Unfortunately, there is insufficient sequence information in the Moore and Haber article to determine how similar the junctions are to the ones we observed. However, these results do confirm that formation of large deletions does not require the absence of Yku80p, and they suggest that, in situations where simple end joining is blocked, large deletions will be more readily recovered among the remaining survivors. Although the Ku complex and the Rad50/Mre11/Xrs2 complex are both involved in NHEJ, mutants lacking one or the other complex often have very different phenotypes (Boulton and Jackson 1996a; Lee *et al.* 1998; Nugent *et al.* 1998; Chen and Kolodner 1999; Chen *et al.* 2001; Grenon *et al.* 2001). It is, therefore, premature to presume that the deletions seen in both sets of experiments represent the same pathway.

Aberrant gene conversions: Another unexpected class of 5-FOA-resistant survivors was the aberrant gene conversions. Given the limited region of homology (60 bases on one side of the cut and 240 on the other side of the cut), this recombination probably occurred by one-sided synthesis-dependent strand annealing that requires direct copying of donor sequence by only one invading strand, reassociation of the extended strand with complementary sequences on the other side of the break, followed by removal of nonhomologous sequences, resynthesis, and religation. In ~1% of conversion events, we observed that the region between homology and nonhomology was not correctly distinguished by the repair machinery, leading to the termination of conversion within a 6-base segment of similar sequence beyond the first mismatch. Mechanisms for distinguishing homology, heterology, and homeology at the termination of a gene conversion event have not been extensively addressed in studies of homologous and homeologous recombination (Bailis and Rothstein 1990; Harris *et al.* 1993; Mezard and Nicolas 1994; Priebe *et al.* 1994; Porter *et al.* 1996), but given our results, it would be worthwhile to use our system to determine whether components of the mismatch repair system are involved in making this distinction.

Insertions: Regarding insertions at DSBs, our data indicate that these events are Ku dependent, providing further support for our previous assertion that insertion of extrachromosomal DNA sequences is a form of NHEJ (Teng *et al.* 1996; Yu and Gabriel 1999). Extrachromosomal DNA insertions at break sites have recently been reported in mammalian cell systems (Sargent *et al.* 1997; Liang *et al.* 1998; Van de Water *et al.* 1998; Lin and Waldman 2001a,b) and plants (Salomon and Puchta 1998; Kirik *et al.* 2000). In each case, the repair events fit the pattern of NHEJ. Thus, the ability to insert available DNA into a break site may be universal and suggests a link between the cellular machinery that degrades DNA and the machinery that repairs breaks in chromosomal DNA. Experiments to examine the generality of the substrates in yeast are underway.

Interactions between repair pathways: An important unanswered question is whether the homologous recombination and NHEJ pathways compete or cooperate in the repair process. By actively binding termini, Ku can focus repair efforts around the original break site, allowing ligation to occur with only minimal overlap between the two ends and with only minimal sequence loss (Dynan and Yoo 1998; Walker *et al.* 2001). After an HO-

induced DSB in yeast, 5′-3′ nucleases create single-stranded 3′ terminal tails that take part in homology searching, presumably aided by Rad52p and other members of the *RAD52* epistasis group (Haber 1995). Single-strand tails are good substrates for initiation of homologous recombination, but they may be less than ideal substrates for NHEJ. Biochemical data suggest that Ku prefers to bind at DSB ends or at double-strand to single-strand junctions, rather than at single-strand tails (Dynan and Yoo 1998). By binding to termini, Ku might block single-strand formation or at least slow it down (Lee *et al.* 1998). Recent articles demonstrate both cooperation and competition in different contexts. A study in yeast suggests a cooperative role for Ku proteins in deletion formation between direct repeats (Cervelli and Galli 2000), while a study in mammalian cells points toward competition between the two pathways in DSB repair (Pierce *et al.* 2001). A yeast study, in which either NHEJ or single-strand annealing could repair a DSB, did not find any evidence of competition between the two pathways (Karathanasis and Wilson 2002).

In wild-type cells we observed that the frequencies of survival by gene conversion and by imprecise end joining were approximately equal. However, the sum of the frequencies of survival in the *rad52* and the *yku80* cells is not equal to the WT frequency, suggesting that there is some synergistic effect when the two pathways are both functional. This is made even more apparent by analyzing the absolute frequency of individual types of repair events in different genetic backgrounds. Insertion frequencies are ~10-fold lower in *rad52* than in WT survivors (3×10^{-5} *vs.* 3×10^{-4}/plated cell), <1-kb deletions are ~5-fold lower (1×10^{-5} *vs.* 5×10^{-5}/plated cell), and larger deletions are ~7-fold lower (3×10^{-6} *vs.* 2×10^{-5}/plated cell), even though Rad52p does not seem to be directly involved in these repair processes. The absence of Rad52p may have a global effect on the repair capacity of the cell after a DSB. On the other hand, the absolute frequency of aberrant gene conversions is equivalent in the *yku80* strain compared to WT (~3×10^{-5}/plated cell) and large deletions are only ~2.5-fold lower (8×10^{-6} *vs.* 2×10^{-5}/plated cell), suggesting that the presence or absence of Yku80p has little to do with the probability of these outcomes. While these data are suggestive, our current results should not be overinterpreted in assessing cooperation or competition between the two pathways. The specific genetic background and genomic context likely influence the speed of single-strand resection, the degree of end protection, and the length of time that cells remain arrested. These, in turn, could affect the efficiency of different repair processes. Despite these caveats, we do not have evidence of competition between the pathways, and there may even be some level of cooperation. More work will be necessary to clarify this situation, including comparison of isogenic strains where the DSB is not subject to both repair pathways, but where all the potential repair proteins are still present.

By examining the frequency and spectrum of repair events after a DSB in different genetic backgrounds, we have begun to appreciate the alternative repair pathways utilized by the cell and we now have the ability to expand the work to examine the effects of different genetic and physical contexts. Using our simple counterselection assay, we can easily generate large numbers of chromosomal rearrangements and analyze their properties. This should prove to be a valuable tool in dissecting mechanisms of double-strand break repair and the causes and consequences of genome instability.

We gratefully acknowledge O. Uzun for providing unpublished strains; S. Brill, M. Gartenberg, J. Haber, and members of the Gabriel laboratory for helpful discussions; and M. Gartenberg and J. L. Souciet for critical comments on the manuscript. This work was funded in part by National Institutes of Health grant CA84098, the New Jersey Commission on Cancer Research, the American Cancer Society, and the Charles and Johanna Busch Endowment.

LITERATURE CITED

Alani, E., L. Cao and N. Kleckner, 1987 A method for gene disruption that allows repeated use of *URA3* selection in the construction of multiply disrupted yeast strains. Genetics **116:** 541–545.

Bailis, A. M., and R. Rothstein, 1990 A defect in mismatch repair in *Saccharomyces cerevisiae* stimulates ectopic recombination between homeologous genes by an excision repair dependent process. Genetics **126:** 535–547.

Belmaaza, A., and P. Chartrand, 1994 One-sided invasion events in homologous recombination at double-strand breaks. Mutat. Res. **314:** 199–208.

Boeke, J. D., F. LaCroute and G. R. Fink, 1984 A positive selection for mutants lacking orotidine-5′-phosphate decarboxylase activity in yeast: 5-fluoro-orotic acid resistance. Mol. Gen. Genet. **197:** 345–346.

Boulton, S. J., and S. P. Jackson, 1996a *Saccharomyces cerevisiae* Ku70 potentiates illegitimate DNA double-strand break repair and serves as a barrier to error-prone DNA repair pathways. EMBO J. **15:** 5093–5103.

Boulton, S. J., and S. P. Jackson, 1996b Identification of a *Saccharomyces cerevisiae* Ku80 homologue: roles in DNA double strand break rejoining and in telomeric maintenance. Nucleic Acids Res. **24:** 4639–4648.

Casaregola, S., H. V. Nguyen, A. Lepingle, P. Brignon, F. Gendre *et al.*, 1998 A family of laboratory strains of *Saccharomyces cerevisiae* carry rearrangements involving chromosomes I and III. Yeast **14:** 551–564.

Cervelli, T., and A. Galli, 2000 Effects of *HDF1* (Ku70) and *HDF2* (Ku80) on spontaneous and DNA damage-induced intrachromosomal recombination in *Saccharomyces cerevisiae*. Mol. Gen. Genet. **264:** 56–63.

Chen, C., and R. D. Kolodner, 1999 Gross chromosomal rearrangements in *Saccharomyces cerevisiae* replication and recombination defective mutants. Nat. Genet. **23:** 81–85.

Chen, C., K. Umezu and R. D. Kolodner, 1998 Chromosomal rearrangements occur in *S. cerevisiae rfa1* mutator mutants due to mutagenic lesions processed by double-strand-break repair. Mol. Cell **2:** 9–22.

Chen, L., K. Trujillo, W. Ramos, P. Sung and A. E. Tomkinson, 2001 Promotion of Dnl4-catalyzed DNA end-joining by the Rad50/Mre11/Xrs2 and Hdf1/Hdf2 complexes. Mol. Cell **8:** 1105–1115.

Clikeman, J. A., G. J. Khalsa, S. L. Barton and J. A. Nickoloff, 2001 Homologous recombinational repair of double-strand breaks in yeast is enhanced by *MAT* heterozygosity through yKU-dependent and -independent mechanisms. Genetics **157:** 579–589.

Codon, A. C., T. Benitez and M. Korhola, 1997 Chromosomal reorganization during meiosis of *Saccharomyces cerevisiae* baker's yeasts. Curr. Genet. **32:** 247–259.

Davis, A. P., and L. S. Symington, 2001 The yeast recombinational repair protein Rad59 interacts with Rad52 and stimulates single-strand annealing. Genetics **159:** 515–525.

Dynan, W. S., and S. Yoo, 1998 Interaction of Ku protein and DNA-dependent protein kinase catalytic subunit with nucleic acids. Nucleic Acids Res. **26:** 1551–1559.

Fasullo, M., P. Dave and R. Rothstein, 1994 DNA-damaging agents stimulate the formation of directed reciprocal translocations in *Saccharomyces cerevisiae*. Mutat. Res. **314:** 121–133.

Fasullo, M. T., and R. W. Davis, 1988 Direction of chromosome rearrangements in *Saccharomyces cerevisiae* by use of *his3* recombinational substrates. Mol. Cell. Biol. **8:** 4370–4380.

Fischer, G., S. A. James, I. N. Roberts, S. G. Oliver and E. J. Louis, 2000 Chromosomal evolution in *Saccharomyces*. Nature **405:** 451–454.

Fishman-Lobell, J., N. Rudin and J. E. Haber, 1992 Two alternative pathways of double-strand break repair that are kinetically separable and independently modulated. Mol. Cell. Biol. **12:** 1292–1303.

Frank-Vaillant, M., and S. Marcand, 2001 NHEJ regulation by mating type is exercised through a novel protein, Lif2p, essential to the ligase IV pathway. Genes Dev. **15:** 3005–3012.

Grenon, M., C. Gilbert and N. F. Lowndes, 2001 Checkpoint activation in response to double-strand breaks requires the Mre11/Rad50/Xrs2 complex. Nat. Cell Biol. **3:** 844–847.

Haber, J. E., 1995 In vivo biochemistry: physical monitoring of recombination induced by site-specific endonucleases. Bioessays **17:** 609–620.

Haber, J. E., and W. Leung, 1996 Lack of chromosome territoriality in yeast: promiscuous rejoining of broken chromosome ends. Proc. Natl. Acad. Sci. USA **93:** 13949–13954.

Harris, S., K. S. Rudnicki and J. E. Haber, 1993 Gene conversions and crossing over during homologous and homeologous ectopic recombination in *Saccharomyces cerevisiae*. Genetics **135:** 5–16.

Hendrickson, E. A., D. G. Schatz and D. T. Weaver, 1988 The scid gene encodes a trans-acting factor that mediates the rejoining event of Ig gene rearrangement. Genes Dev. **2:** 817–829.

Hoffman, C. S., and F. Winston, 1987 A ten-minute DNA preparation from yeast efficiently releases autonomous plasmids for transformation of *Escherichia coli*. Gene **57:** 267–272.

Karathanasis, E., and T. E. Wilson, 2002 Enhancement of *Saccharomyces cerevisiae* end-joining efficiency by cell growth stage but not by impairment of recombination. Genetics **161:** 1015–1027.

Kegel, A., J. O. Sjostrand and S. U. Astrom, 2001 Nej1p, a cell type-specific regulator of nonhomologous end joining in yeast. Curr. Biol. **11:** 1611–1617.

Kirik, A., S. Salomon and H. Puchta, 2000 Species-specific double-strand break repair and genome evolution in plants. EMBO J. **19:** 5562–5566.

Kramer, K. M., J. A. Brock, K. Bloom, J. K. Moore and J. E. Haber, 1994 Two different types of double-strand breaks in *Saccharomyces cerevisiae* are repaired by similar *RAD52* independent, nonhomologous recombination events. Mol. Cell. Biol. **14:** 1293–1301.

Kraus, E., W. Y. Leung and J. E. Haber, 2001 Break-induced replication: a review and an example in budding yeast. Proc. Natl. Acad. Sci. USA **98:** 8255–8262.

Lee, S. E., J. K. Moore, A. Holmes, K. Umezu, R. D. Kolodner *et al.*, 1998 *Saccharomyces* Ku70, mre11/rad50 and RPA proteins regulate adaptation to G2/M arrest after DNA damage. Cell **94:** 399–409.

Legoix, P., H. D. Sarkissian, L. Cazes, S. Giraud, F. Sor *et al.*, 2000 Molecular characterization of germline NF2 gene rearrangements. Genomics **65:** 62–66.

Lewis, L. K., and M. A. Resnick, 2000 Tying up loose ends: nonhomologous end-joining in *Saccharomyces cerevisiae*. Mutat. Res. **451:** 71–89.

Liang, F., and M. Jasin, 1996 Ku80-deficient cells exhibit excess degradation of extrachromosomal DNA. J. Biol. Chem. **271:** 14405–14411.

Liang, F., M. Han, P. J. Romanienko and M. Jasin, 1998 Homology-directed repair is a major double-strand break repair pathway in mammalian cells. Proc. Natl. Acad. Sci. USA **95:** 5172–5177.

Lin, Y., and A. S. Waldman, 2001a Capture of DNA sequences at double-strand breaks in mammalian chromosomes. Genetics **158:** 1665–1674.

Lin, Y., and A. S. Waldman, 2001b Promiscuous patching of broken chromosomes in mammalian cells with extrachromosomal DNA. Nucleic Acids Res. **29:** 3975–3981.

Manivasakam, P., S. C. Weber, J. McElver and R. H. Schiestl, 1995 Micro-homology mediated PCR targeting in *Saccharomyces cerevisiae*. Nucleic Acids Res. **23:** 2799–2800.

Mezard, C., and A. Nicolas, 1994 Homologous, homeologous, and illegitimate repair of double-strand breaks during transformation of a wild-type strain and a *rad52* mutant strain of *Saccharomyces cerevisiae*. Mol. Cell. Biol. **14:** 1278–1292.

Moore, J. K., and J. E. Haber, 1996a Cell cycle and genetic requirements of two pathways of nonhomologous end-joining repair of double-strand breaks in *Saccharomyces cerevisiae*. Mol. Cell. Biol. **16:** 2164–2173.

Moore, J. K., and J. E. Haber, 1996b Capture of retrotransposon DNA at the sites of chromosomal double-strand breaks. Nature **383:** 644–646.

Myung, K., A. Datta and R. D. Kolodner, 2001 Suppression of spontaneous chromosomal rearrangements by S phase checkpoint functions in Saccharomyces cerevisiae. Cell **104:** 397–408.

Nugent, C. I., G. Bosco, L. O. Ross, S. K. Evans, A. P. Salinger *et al.*, 1998 Telomere maintenance is dependent on activities required for end repair of double-strand breaks. Curr. Biol. **8:** 657–660.

Ochman, H., A. S. Gerber and D. L. Hartl, 1988 Genetic applications of an inverse polymerase chain reaction. Genetics **120:** 621–623.

Ooi, S. L., D. D. Shoemaker and J. D. Boeke, 2001 A DNA microarray-based genetic screen for nonhomologous end-joining mutants in *Saccharomyces cerevisiae*. Science **294:** 2552–2556.

Paques, F., and J. E. Haber, 1997 Two pathways for removal of nonhomologous DNA ends during double-strand break repair in *Saccharomyces cerevisiae*. Mol. Cell. Biol. **17:** 6765–6771.

Paques, F., and J. E. Haber, 1999 Multiple pathways of recombination induced by double-strand breaks in *Saccharomyces cerevisiae*. Microbiol. Mol. Biol. Rev. **63:** 349–404.

Paques, F., W. Y. Leung and J. E. Haber, 1998 Expansions and contractions in a tandem repeat induced by double-strand break repair. Mol. Cell. Biol. **18:** 2045–2054.

Pierce, A. J., P. Hu, M. Han, N. Ellis and M. Jasin, 2001 Ku DNA end-binding protein modulates homologous repair of double-strand breaks in mammalian cells. Genes Dev. **15:** 3237–3242.

Porter, G., J. Westmoreland, S. Priebe and M. A. Resnick, 1996 Homologous and homeologous intermolecular gene conversion are not differentially affected by mutations in the DNA damage or the mismatch repair genes *RAD1*, *RAD50*, *RAD51*, *RAD52*, *RAD54*, *PMS1*, and *MSH2*. Genetics **143:** 755–767.

Potier, S., B. Winsor and F. Lacroute, 1982 Genetic selection for reciprocal translocation at chosen chromosomal sites in *Saccharomyces cerevisiae*. Mol. Cell. Biol. **2:** 1025–1032.

Priebe, S. D., J. Westmoreland, T. N. Tillgren and M. A. Resnick, 1994 Induction of recombination between homologous and diverged DNAs by double-strand gaps and breaks and role of mismatch repair. Mol. Cell. Biol. **14:** 4802–4814.

Ricchetti, M., C. Fairhead and B. Dujon, 1999 Mitochondrial DNA repairs double-strand breaks in yeast chromosomes. Nature **402:** 96–100.

Rothkamm, K., M. Kuhne, P. A. Jeggo and M. Lobrich, 2001 Radiation-induced genomic rearrangements formed by nonhomologous end-joining of DNA double-strand breaks. Cancer Res. **61:** 3886–3893.

Salomon, S., and H. Puchta, 1998 Capture of genomic and T-DNA sequences during double-strand break repair in somatic plant cells. EMBO J. **17:** 6086–6095.

Sargent, R. G., M. A. Brenneman and J. H. Wilson, 1997 Repair of site-specific double-strand breaks in a mammalian chromosome by homologous and illegitimate recombination. Mol. Cell. Biol. **17:** 267–277.

Schiestl, R., and T. D. Petes, 1991 Integration of DNA fragments by illegitimate recombination in *Saccharonmyces cerevisiae*. Proc. Natl. Acad. Sci. USA **88:** 7585–7589.

Schiestl, R. H., 1989 Nonmutagenic carcinogens induce intrachromosomal recombination in yeast. Nature **337:** 285–288.

Schiestl, R. H., M. Dominska and T. D. Petes, 1993 Transforma-

tion of *Saccharomyces cerevisiae* with non-homologous DNA: illegitimate integration of transforming DNA into yeast chromosomes and *in vivo* ligation of transforming DNA to mitochondrial DNA sequences. Mol. Cell. Biol. **13:** 2697–2705.

Schiestl, R. H., J. Zhu and T. D. Petes, 1994 Effect of mutations in genes affecting homologous recombination on restriction enzyme-mediated and illegitimate recombination in *Saccharomyces cerevisiae*. Mol. Cell. Biol. **14:** 4493–4500.

Schuler, W., I. J. Weiler, A. Schuler, R. A. Phillips, N. Rosenberg *et al.*, 1986 Rearrangement of antigen receptor genes is defective in mice with severe combined immune deficiency. Cell **46:** 963–972.

Sherman, F., G. R. Fink and J. B. Hicks, 1986 *Methods in Yeast Genetics: A Laboratory Manual*. Cold Spring Harbor Laboratory Press, Cold Spring Harbor, NY.

Sikorski, R. S., and J. D. Boeke, 1991 In vitro mutagenesis and plasmid shuffling: from cloned gene to mutant yeast. Methods Enzymol. **194:** 302–318.

Sugawara, N., and J. W. Szostak, 1983 Recombination between sequences in nonhomologous positions. Proc. Natl. Acad. Sci. USA **80:** 5675–5679.

Sugawara, N., G. Ira and J. E. Haber, 2000 DNA length dependence of the single-strand annealing pathway and the role of *Saccharomyces cerevisiae RAD59* in double-strand break repair. Mol. Cell. Biol. **20:** 5300–5309.

Taccioli, G. E., G. Rathbun, E. Oltz, T. Stamato, P. A. Jeggo *et al.*, 1993 Impairment of V(D)J recombination in double-strand break repair mutants. Science **260:** 207–210.

Teng, S. C., B. Kim and A. Gabriel, 1996 Retrotransposon reverse-transcriptase-mediated repair of chromosomal breaks. Nature **383:** 641–644.

Umezu, K., M. Hiraoka, M. Mori and H. Maki, 2002 Structural analysis of aberrant chromosomes that occur spontaneously in diploid *Saccharomyces cerevisiae*: retrotransposon Ty1 plays a crucial role in chromosomal rearrangements. Genetics **160:** 97–110.

Valencia, M., M. Bentele, M. B. Vaze, G. Herrmann, E. Kraus *et al.*, 2001 NEJ1 controls non-homologous end joining in *Saccharomyces cerevisiae*. Nature **414:** 666–669.

Van de Water, N., R. Williams, P. Ockelford and P. Browett, 1998 A 20.7 kb deletion within the factor VIII gene associated with LINE-1 element insertion. Thromb. Haemostasis **79:** 938–942.

Verkaik, N. S., R. E. Esveldt-van Lange, D. van Heemst, H. T. Bruggenwirth, J. H. Hoeijmakers *et al.*, 2002 Different types of V(D)J recombination and end-joining defects in DNA double-strand break repair mutant mammalian cells. Eur. J. Immunol. **32:** 701–709.

Wach, A., A. Brachat, R. Pohlmann and P. Philippsen, 1994 New heterologous modules for classical or PCR-based gene disruptions in *Saccharomyces cerevisiae*. Yeast **10:** 1793–1808.

Walker, J. R., R. A. Corpina and J. Goldberg, 2001 Structure of the Ku heterodimer bound to DNA and its implications for double-strand break repair. Nature **412:** 607–614.

Welcker, A. J., J. de Montigny, S. Potier and J. L. Souciet, 2000 Involvement of very short DNA tandem repeats and the influence of the *RAD52* gene on the occurrence of deletions in *Saccharomyces cerevisiae*. Genetics **156:** 549–557.

Wiemels, J. L., and M. Greaves, 1999 Structure and possible mechanisms of TEL-AML1 gene fusions in childhood acute lymphoblastic leukemia. Cancer Res. **59:** 4075–4082.

Woods-Samuels, P., H. H. J. Kazazian and S. E. Antonarakis, 1991 Nonhomologous recombination in the human genome: deletions in the human factor VIII gene. Genomics **10:** 94–101.

Yu, X., and A. Gabriel, 1999 Patching broken chromosomes with extranuclear cellular DNA. Mol. Cell **4:** 873–881.

Communicating editor: G. R. Smith